Article

# Formation and Characterization of Protein–Protein Complexes in Vacuo

J. Mitchell Wells, Paul A. Chrisman, and Scott A. McLuckey

*J. Am. Chem. Soc.*, **2003**, 125 (24), 7238-7249• DOI: 10.1021/ja035051l • Publication Date (Web): 20 May 2003



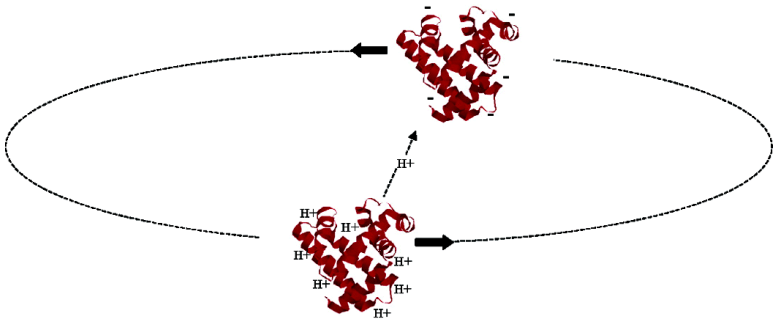


## More About This Article

Additional resources and features associated with this article are available within the HTML version:

- Supporting Information
- Links to the 3 articles that cite this article, as of the time of this article download
- Access to high resolution figures
- Links to articles and content related to this article
- Copyright permission to reproduce figures and/or text from this article

View the Full Text HTML

J|A|C|S
ARTICLES
Published on Web 05/20/2003

# Formation and Characterization of Protein−Protein Complexes in Vacuo

J. Mitchell Wells, Paul A. Chrisman, and Scott A. McLuckey*

*Contribution from the Department of Chemistry, Purdue University, West Lafayette, Indiana 47907-2084*

Received March 7, 2003; Revised Manuscript Received April 7, 2003; E-mail: mcluckey@purdue.edu

***Abstract:*** Gas-phase reactions between multiply charged positive and negative protein ions are carried out in a quadrupole ion trap mass spectrometer. The ions react with one another by proton transfer and complex formation. Proton transfer products and complexes are formed via competitive processes in single ion/ion encounters. The relative contributions of proton transfer versus complex formation are dependent upon the charges of the ions as well as other characteristics of the ions yet to be clearly delineated. No fragmentation of covalent bonds of the protein reactants is observed. A model that considers the trajectories associated with ion/ion interactions appears to hold the most promise in accounting for the results. The formation of bound ion/ion orbits appears to play an important role in determining overall reaction kinetics as well as the distribution of ion/ion reaction products. Tandem mass spectrometry is used to compare protein complexes formed in the gas-phase with those formed initially in solution and subsequently liberated by electrospray; it is shown that both forms of complex dissociate similarly, but the complexes formed in the gas phase can retain a "memory" of their method of formation.

## Introduction

The study of the interactions of proteins with other proteins is a longstanding activity given that proteins often perform their functions as members of protein complexes. With the recent generation of whole genome data, the study of protein−protein interactions has become particularly relevant to the determination of gene function. Over the course of the past decade, it has been demonstrated by many groups that it is possible to preserve noncovalently bound protein complexes as gaseous ions[1] via electrospray ionization.[2] This is a noteworthy development in that it has enabled the tools of mass spectrometry to be applied directly to protein complexes. For example, it allows for the measurement of the mass of the complex with a degree of precision and accuracy not available with other approaches and also allows for the application of tandem mass spectrometry to protein complexes to derive structural and energetic information.[3] The study of gas-phase protein complexes expands upon the active study of the gas-phase structures and stabilities of gaseous protein ions through such approaches as ion mobility[4] and collision cross-section[5] measurements, ion/molecule reactions,[6] and unimolecular dissociation.[7] Of particular interest is the relationship between the structures and stabilities of gaseous protein ions and their complexes relative to those found in solution. This issue has given rise to the study of partially solvated protein ions in the gas-phase.[8]

The study of protein complexes in the gas phase presents unique challenges relative to the study of individual protein subunits. For example, it can be difficult to form and preserve gaseous complex ions in sufficient numbers to allow for application of some of the techniques developed to study intact protein ions. Furthermore, protein complexes are usually observed with relatively low numbers of charges such that the mass-to-charge ratios of the complex ions are relatively high. In some cases, this tends to restrict the tools amenable to study

(1) (a) Ganem, B.; Li, Y. T.; Henion, J. D. *J. Am. Chem. Soc.* **1991**, *113*, 7818−7819. (b) Loo, J. A. *Int. J. Mass Spectrom.* **2000**, *200*, 175−186. (c) Light-Wahl, K. J.; Schwartz, B. L.; Smith, R. D. *J. Am. Chem. Soc.* **1994**, *116*, 5271−5278. (d) Benjamin, D. R.; Robinson, C. V.; Hendrick, J. P.; Hartl, F. U.; Dobson, C. M. *Proc. Natl. Acad. Sci. U.S.A.* **1998**, *95*, 391−7395. (e) Siuzdak, G.; Bothner, B.; Yeager, M.; Brugidou, C.; Fauquet, C. M.; Hoey, K.; Chang, C. M. *Chem. Biol.* **1996**, *3*, 45−48. (f) Tito, M. A.; Tars, K.; Valegard, K.; Hajdu, J.; Robinson, C. V. *J. Am. Chem. Soc.* **2000**, *122*, 3550−3551. (g) Robinson, C. V. *Nat. Struct. Biol.* **2002**, *9*, 505−506. (h) Kitova, E. N.; Bundle, D. R.; Klassen, J. S. *J. Am. Chem. Soc.* **2002**, *124*, 9340−9341.

(2) Fenn, J. B.; Mann, M.; Meng, C. K.; Wong, S. F.; Whitehouse, C. M. *Science* **1989**, *246*, 64−71.

(3) (a) Versluis, C.; Heck, A. J. R. *Int. J. Mass Spectrom.* **2001**, *210*, 637−649. (b) Hunter, C. L.; Mauk, A. G.; Douglas, D. J. *Biochemistry* **1997**, *36*, 1018−1025. (c) Gross, D. S.; Zhao, Y. X.; Williams, E. R. *J. Am. Soc. Mass Spectrom.* **1997**, *8*, 519−524. (d) Rostom, A. A.; Fucini, P.; Benjamin, D. R.; Juenemann, R.; Nierhaus, K. H.; Hartl, F. U.; Dobson, C. M.; Robinson, C. V. *Proc. Natl. Acad. Sci. U.S.A.* **2000**, *97*, 5185−5190. (e) Felitsyn, N.; Kitova, E. N.; Klassen, J. S. *Anal. Chem.* **2001**, *73*, 4647−4661. (f) Schwartz, B. L.; Bruce, J. E.; Anderson, G. A.; Hofstadler, S. A.; Rockwood, A. L.; Smith, R. D.; Chilkoti, A.; Stayton, P. S. *J. Am. Soc. Mass Spectrom.* **1995**, *6*, 459−465. (g) Smith, R. D.; Light-Wahl, K. J.; Winger, B. E.; Loo, J. A. *Org. Mass Spectrom.* **1992**, *27*, 811−821. (h) Fitzgerald, M. C.; Chernushevich, I.; Standing, K. G.; Whitman, C. P.; Kent, S. B. H. *Proc. Natl. Acad. Sci. U.S.A.* **1996**, *93*, 6851−6856. (i) Rostom, A. A.; Sunde, M.; Richardson, S. J.; Schreiber, G.; Jarvis, S.; Bateman, R.; Dobson, C. M.; Robinson, C. V. *Proteins: Struct. Func. Gen.* **1998**, 3−11. (j) Versluis, C.; van der Staaij, A.; Stokvis, E.; Heck, A. J. R.; de Craene, B. *J. Am. Soc. Mass Spectrom.* **2001**, *12*, 329−336. (k) Zhang, Z. G.; Krutchinsky, A.; Endicott, S.; Realini, C.; Rechsteiner, M.; Standing, K. G. *Biochemistry* **1999**, *38*, 5651−5658.

(4) (a) Von Helden, G.; Wyttenbach, T.; Bowers, M. T. *Science* **1995**, *267*, 1483−1485. (b) Clemmer, D. E.; Jarrold, M. F. *J. Mass Spectrom.* **1997**, *32*, 577−592. (c) Shelimov, K. B.; Jarrold, M. F. *J. Am. Chem. Soc.* **1997**, *119*, 2987−2994.

(5) (a) Covey, T. R.; Douglas, D. J. *J. Am. Soc. Mass Spectrom.* **1993**, *4*, 616−623. (b) Chen, Y.-L.; Collings, B. A.; Douglas, D. J. *J. Am. Soc. Mass Spectrom.* **1997**, *8*, 681−687.


**10.1021/ja035051l CCC: $25.00** 

of protein complexes to those capable of mass analysis of ions with mass-to-charge rations greater than about 5000. Therefore, although there is much yet to be learned about individual gaseous protein ions,[9] even less is known about gaseous protein complexes. For this reason, it is desirable to apply to charged protein complexes the tools and methodologies developed for the study of large covalently bound ions and to develop new approaches to address issues that are unique to noncovalently bound complexes. These issues include, for example, the nature of the interactions between complex subunits in the condensed and gas phases.

In a preliminary report, we described a means for forming ionized protein complexes in vacuo via the reaction of individual protein subunits of opposite charge.[10] Ion/ion reactions have already been demonstrated to be useful for charge state manipulation of protein ions[11] and for product ions formed by dissociation of protein precursor ions.[12] When ion/ion reactions are effected in a quadrupole ion trap, they can be employed between mass selection steps as part of a multistep process involving several ion reaction periods.[13] A particularly useful application of ion/ion reactions in an ion trap is the concentration of most or all charge states of a protein formed initially by electrospray into a single charge state.[14] This technique, referred to as ion parking, has been used to concentrate and charge-state-purify protein ions present in a complex mixture for subsequent collision-induced dissociation and charge state manipulation of the product ions via ion/ion reactions to simplify spectral interpretation.[15] This process has been demonstrated to enable protein identification from mixtures comprised of dozens of protein components. The formation of adduct or complex ions is undesirable when the objective is to manipulate charge states for ion parking and for simplifying product ion spectra. Charge state manipulation of protein cations via proton transfer is straightforward with anions derived from glow discharge of perfluorocarbons,[16] as no such adducts are formed. However, when proteins of opposite charge are used as reactants, the formation of condensation products is a major reaction channel.

The ability to form protein complexes in the gas phase provides a potentially useful new capability in the study of protein complexes formed initially in solution and subsequently ionized by electrospray. It enables a degree of specificity in the synthesis of protein complexes that is not available in the condensed phase. For example, protein subunits can be mass and charge state selected for reaction leading to a high degree of dimensionality in options for producing a complex of a given composition and charge. Furthermore, information about the structures and stabilities of gaseous protein ions, which serve as subunits for the synthesis of protein complexes, can be useful in defining the characteristics of the building blocks, in addition to mass and charge, in the formation of complex ions. Nominally identical complexes formed in solution and in vacuo can then be subjected to similar probes and compared. The ability to synthesize complexes via different routes in the gas phase can therefore provide novel insights into the structures and stabilities of complexes formed originally in solution. This paper provides a full account of the phenomenology associated with the reactions of oppositely charged anhydrous proteins in the gas phase in an ion trap. It includes a discussion of the dynamics of the reactions as they relate to the various products formed and also relates results of the collision-induced dissociation of the protein−protein complexes formed in solution and several complexes of the same composition and total charge formed in various ways in the gas phase.

## Experimental Section

The experiments reported herein were performed using a modified Finnigan (San Jose, CA) Ion Trap Mass Spectrometer (ITMS) which has been described in detail elsewhere.[17] Briefly, the instrument consists of a quadrupole ion trap fitted with two electrospray ionization sources, mounted 180° to one another and 90° to the axial dimension of the ion trap. A DC turning quadrupole allows sequential injection of opposite polarity ions from the two ESI sources into the ion trap under control of the ion trap software.

All proteins were obtained from Sigma (St. Louis, MO) and were used without further purification. Nano-electrospray (nano-ES) ionization from drawn borosilicate glass capillaries was used to produce both

(6) (a) Green, M. K.; Lebrilla, C. B. *Mass Spectrom. Rev.* **1997**, *16*, 53−71. (b) McLuckey, S. A.; Van Berkel, G. J.; Glish, G. L. *J. Am. Chem. Soc.* **1990**, *112*, 5668−5670. (c) Ogorzalek Loo, R. R.; Loo, J. A.; Udseth, H. R.; Fulton, J. L.; Smith, R. D. *Rapid Commun. Mass Spectrom.* **1992**, *6*, 159−165. (d) Ogorzalek Loo, R. R.; Smith, R. D. *J. Mass Spectrom.* **1995**, *30*, 339−347. (e) Williams, E. R. *J. Mass Spectrom.* **1996**, *31*, 831−842. (f) Winger, B. E.; Light-Wahl, K. J.; Rockwood, A. L.; Smith, R. D. *J. Am. Chem. Soc.* **1992**, *114*, 5897−5898. (g) Wood, T. D.; Chorush, R. A.; Wampler, F. M., III; Little, D. P.; O'Connor, P. B.; McLafferty, F. W. *Proc. Natl. Acad. Sci. U.S.A.* **1995**, *92*, 2451−2454. (h) Suckau, D.; Shi, Y.; Beu, S. C.; Senko, M. W.; Quinn, J. P.; Wampler, F. M., III; McLafferty, F. W. *Proc. Natl. Acad. Sci. U.S.A.* **1993**, *90*, 790−793. (i) McLafferty, F. W.; Guan, Z. Q.; Haupts, U.; Wood, T. D.; Kelleher, N. L. *J. Am. Chem. Soc.* **1998**, *120*, 4732−4740. (j) Campbell, S.; Rodgers, M. T.; Marzluff, E. M.; Beauchamp, J. L. *J. Am. Chem. Soc.* **1995**, *117*, 12 840−12 854. (k) Wyttenbach, T.; Bowers, M. T. *J. Am. Soc. Mass Spectrom.* **1999**, *10*, 9−14. (l) Schaaff, T. G.; Stephenson, J. L., Jr.; McLuckey, S. A *J. Am. Chem. Soc.* **1999**, *121*, 8907−8919. (m) Schaaff, T. G.; Stephenson, J. L., Jr.; McLuckey, S. A. *J. Am. Soc. Mass Spectrom.* **2000**, *11*, 167−171. (n) Schaaff, T. G.; Stephenson, J. L., Jr.; McLuckey, S. A. *Int. J. Mass Spectrom.* **2000**, *202*, 299−313.

(7) (a) Beu, S. C.; Senko, M. W.; Quinn, J. P.; Wampler, F. M., III; McLafferty, F. W. *J. Am. Soc. Mass Spectrom.* **1993**, *4*, 557−565. (b) Senko, M. W.; Speir, J. P.; McLafferty, F. W. *Anal. Chem.* **1994**, *66*, 2801−2808. (c) Little, D. P.; Speir, J. P.; Senko, M. W.; O'Connor, P. B.; McLafferty, F. W. *Anal. Chem.* **1994**, *66*, 2809−2815. (d) Horn, D. M.; Zubarev, R. A.; McLafferty, F. W. *Proc. Natl Acad. Sci. U.S.A.* **2000**, *97*, 10 313−10 317. (e) Horn, D. M.; Breuker, K.; Frank, A. J.; McLafferty, F. W. *J. Am. Chem. Soc.* **2001**, *123*, 9792−9799. (f) Oh, H. B.; Breuker, K.; Sze, S. K.; Ge, Y.; Carpenter, B. K.; McLafferty, F. W. *Proc. Natl. Acad. Sci. U.S.A.* **2002**, *99*, 15 863−15 868. (g) Price, W. D.; Schnier, P. D.; Williams, E. R. *Anal. Chem.* **1996**, *68*, 859−866. (h) Price, W. D.; Williams, E. R. *J. Phys. Chem. A* **1997**, *101*, 8844−8852.

(8) (a) Lee, S. W.; Freivogel, P.; Schindler, T.; Beauchamp, J. L. *J. Am. Chem. Soc.* **1998**, *120*, 11 758−11 765. (b) Rodriguez-Cruz, S. E.; Klassen, J. S.; Williams, E. R. *J. Am. Soc. Mass Spectrom.* **1999**, *10*, 958−968.

(9) Hoaglund-Hyzer, C. S.; Counterman, A. E.; Clemmer, D. E. *Chem. Rev.* **1999**, *99*, 3037−3079.

(10) Wells, J. M.; Chrisman, P. A.; McLuckey, S. A. *J. Am. Chem. Soc.* **2001**, *123*, 12 428−12 429.

(11) (a) Stephenson, J. L., Jr.; McLuckey, S. A. *J. Am. Chem. Soc.* **1996**, *118*, 7390−7397. (b) Stephenson, J. L., Jr.; McLuckey, S. A. *Anal. Chem.* **1996**, *68*, 4026−4032. (c) Stephenson, J. L., Jr.; McLuckey, S. A. *J. Am. Soc. Mass Spectrom.* **1998**, *9*, 585−596. (d) Stephenson, J. L., Jr.; McLuckey, S. A. *J. Mass Spectrom.* **1998**, *33*, 664−672. (e) Scalf, M.; Westphall, M. S.; Krause, J.; Kaufman, S. L.; Smith, L. M. *Science* **1999**, *283*, 194−197. (f) Scalf, M.; Westphall, M. S.; Smith, L. M. *Anal. Chem.* **2000**, *72*, 52−60.

(12) (a) Stephenson, J. L., Jr.; McLuckey, S. A. *Anal. Chem.* **1998**, *70*, 3533−3544. (b) Cargile, B. J.; McLuckey, S. A.; Stephenson, J. L., Jr. *Anal. Chem.* **2001**, *74*, 1277−1285. (c) Engel, B. J.; Pan, P.; Reid, G. E.; Wells, J. M.; McLuckey, S. A. *Int. J. Mass Spectrom.* **2002**, *219*, 171−187. (d) Chrisman, P. A.; Newton, K. A.; Wells, J. M.; Reid, G. E.; McLuckey, S. A. *Int. J. Mass Spectrom.* **2001**, *212*, 359−376. (e) Reid, G. E.; Wu, J.; Chrisman, P. A.; Wells, J. M.; McLuckey, S. A. *Anal. Chem.* **2001**, *73*, 3274−3281.

(13) McLuckey, S. A.; Wells, J. M.; Stephenson, J. L., Jr.; Goeringer, D. E. *Int. J. Mass Spectrom.* **2000**, *200*, 137−161.

(14) McLuckey, S. A.; Reid, G. E.; Wells, J. M. *Anal. Chem.* **2002**, *74*, 336−346.

(15) Reid, G. E.; Shang, H.; Hogan, J. M.; Lee, G. U.; McLuckey, S. A. *J. Am. Chem. Soc.* **2002**, *124*, 7353−7362.

(16) McLuckey, S. A.; Stephenson, J. L., Jr. *Mass Spectrom. Rev.* **1998**, *17*, 369−407.

(17) Wells, J. M.; Chrisman, P. A.; McLuckey, S. A. *J. Am. Soc. Mass Spectrom.* **2002**, *13*, 614−622.

positive and negative protein ions.[18] For positive ions, protein solutions of approximately 0.1 mg/mL were prepared in 1% aqueous acetic acid or in 50% methanol/49% water/1% acetic acid. For negative ions, protein solutions of approximately 0.1 mg/mL were prepared in 5 mM aqueous ammonium bicarbonate. 10−20 $\mu$L of these solutions were loaded into a nano-ES capillary, and a stainless steel wire to which 1−1.5 kV of the appropriate polarity was applied was inserted into the solution to effect nano-ES at a flow rate of roughly 50 nL/min. To generate solution-phase protein dimers, nano-ES of 1 mg/mL protein was performed from solutions prepared in pure water. The charge states of the solution-phase dimers were manipulated via ion/ion reactions with singly charged anions of perfluorodimethylcyclohexane (PDCH) generated from a corona discharge source used in place of one of the ES sources.[17]

For the gas-phase ion/ion reactions of opposite polarity protein ions, positive ions of the protein under study were injected into the ion trap and the desired charge state was isolated using amplitude ramps of the trapping radio frequency (RF) voltage applied to the ion trap ring electrode, combined with resonance ejection voltages applied across the ion trap end caps at the appropriate frequencies.[19] Negative ions were then injected into the ion trap and isolated with resonance ejection RF amplitude ramps. Isolation of the second population of ions injected into the ion trap must be done without ejection of the isolated ion population from the previous ion accumulation period. This can be done with the judicious selection of ion isolation ramps provided there are no unwanted ions of one ion polarity at the same mass-to-charge ratio as a reactant ion of interest of the other polarity. In the data shown here, conditions could be established to avoid undesirable overlaps in mass-to-charge ratio of oppositely charged ions. However, ion/ion reactions can proceed while ions of the second injected ion population are being accumulated. This can be minimized by use of relatively short ion injection periods combined with the application of a single resonance ejection frequency to eject the most abundant unwanted ion of the ion polarity being injected. For the work reported here, the product ion spectra primarily show products resulting from the reaction of two isolated protein ion charge states, with minimal contributions due to side reactions occurring during the anion injection and isolation period. Mutual storage and ion/ion reactions were carried out for variable reactions times at an ion trap low mass cutoff (LMCO) value of 400. Dissociation of the protein/protein complexes was performed by isolating the complex with resonance ejection RF amplitude ramps, followed by resonance excitation and collision-induced dissociation (CID) of the ions via application of the appropriate frequency across the ion trap end caps. Mass analysis was performed by ramping the amplitude of the applied RF trapping voltage while simultaneously applying a resonance ejection voltage across the end caps at a frequency chosen to give the desired mass-to-charge range.[20] All data reported here were collected with approximately 1 mTorr of helium bath gas added to the vacuum manifold. This bath gas provides collisional cooling of the injected ions, and serves as collision gas for the collision-induced dissociation experiments.

## Results and Discussion

**Reaction Phenomenology.** The phenomena associated with the reactions of multiply protonated proteins with multiply deprotonated proteins are illustrated with ions derived from cytochrome *c* (C) and bovine ubiquitin (U). Several of these phenomena were described in the original communication but further elaboration is given here. Figure 1 shows typical spectra obtained from an ion/ion reaction involving oppositely charged proteins. Figure 1a shows the positive post-ion/ion reaction spectrum of the 8+ ion of bovine cytochrome *c* in reaction with the 5- ion of C.[21] Figure 1b shows the negative post-ion/ion reaction spectrum obtained under the same reaction conditions. The positive product ion spectrum is typical of results obtained from the reaction of protein cations with protein anions when the positive ion charge state is greater than that of the negative ion. Products due to transfer of varying numbers of protons from the positive to the negative protein ions are observed along with a protein−protein complex of charge equal to the sum of the reactant charges. Both proton transfer and complex formation are observed for all protein and charge state combinations studied, although the relative contributions of proton transfer and complex formation can vary widely with charge state and protein identity, as discussed below. Figure 1b is typical of negative ion data when the anion charge state is less than that of the positive ion. Proton-transfer products are observed but no complex formation is evident because the net charge of the complex is positive. In the case of the experiment leading to Figure 1, the complementary proton-transfer products are $C^{7+}/C^{4-}$, $C^{6+}/C^{3-}$, $C^{5+}/C^{2-}$, $C^{4+}/C^{-}$, $C^{3+}/C^{0}$, and $C^{2+}/C^{+}$. All of the possible product ions are observed between the two spectra of Figure 1. The abundances of the various possible proton-transfer products go through a maximum for the $C^{5+}/C^{2-}$ and $C^{4+}/C^{-}$ complementary pairs. When the areas under the peaks and detector discrimination as a function of charge state are considered, the relative abundances of the various charge states in each spectrum are consistent with their complementary products in the other spectrum. There is no evidence in either spectrum for fragmentation of covalent bonds of the protein ions.

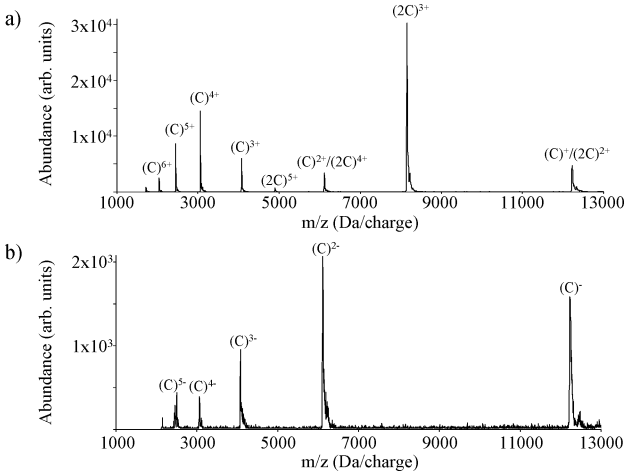


***Figure 1.*** Product ion spectra illustrating the results of an ion/ion reaction between 8+ and 5− ions of bovine cytochrome *c* (C). (a) positive product ions resulting from a 100 ms reaction. (b) corresponding negative product ions obtained under the same reaction conditions as (a).

With the exception of spectra acquired after short mutual storage times, as discussed further below, the relative abun-

(18) (a) Fong, K. W. Y.; Chan, T.-W. D.; *J. Am. Soc. Mass Spectrom.* **1999**, *10*, 72−75. (b) Van Berkel, G. J.; Asano, K. G.; Schnier, P. D. *J. Am. Soc. Mass Spectrom.* **2001**, *12*, 853−862.

(19) McLuckey, S. A.; Goeringer, D. E.; Glish, G. L. *J. Am. Soc. Mass Spectrom.* **1991**, *2*, 11−21.

(20) (a) Kaiser, R. E., Jr.; Louris, J. N.; Amy, J. W.; Cooks, R. G. *Rapid Commun. Mass Spectrom.* **1989**, *3*, 225−229. (b) Kaiser, R. E., Jr.; Cooks, R. G.; Stafford, G. C., Jr.; Syka, J. E. P.; Hemberger, P. H. *Int. J. Mass Spectrom. Ion Processes* **1991**, *106*, 79−115.

(21) Under the ES conditions used to form the positive ions, cytochrome *c* is expected to be in the oxidized form such that one of the excess positive charges arises from the iron III associated with the heme group. Wells, J. M.; Reid, G. E.; Engel, B. J.; Pan, P.; McLuckey, S. A. *J. Am. Soc. Mass Spectrom.* **2001**, *12*, 873−876. Throughout this manuscript, protein ions are indicated by charge and, with the exception of the charged heme group, excess charges are accounted for either by protonation (cations) or deprotonation (anions).

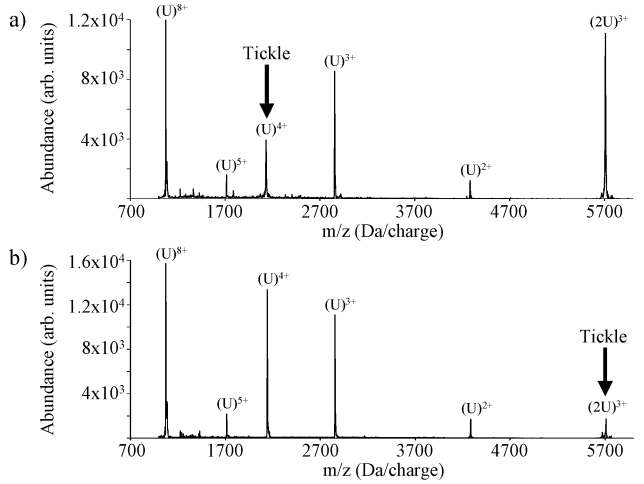


***Figure 2.*** Product ion spectra illustrating the results of ion/ion reactions between 8+ and 5− ions of ubiquitin (U), with resonance excitation voltages ("tickles") applied to selectively remove certain products during the ion/ion reaction period. (a) The 4+ proton-transfer product ($U^{4+}$) is partially removed. (b) The protein−protein complex product ($2U^{3+}$) is removed.

dances of the products in the post-ion/ion reaction spectra are independent of reaction time up to about 100 ms. The reactant ion abundances decrease with time while all of the major product ions increase proportionately in abundance. At long reaction times (roughly 100 ms or greater), low abundance signals begin to appear that result from ion/ion reactions of first generation product ions with the oppositely charged reactant ions. However, under the conditions of the experiments reported here, the major product ions arise from single ion/ion encounters. Several "knockout" experiments were conducted to examine the relationship between the proton transfer and complex products. These experiments involved the application of a relatively large amplitude sine-wave in dipolar fashion to the end-cap electrodes of the frequency of a selected product ion during the ion/ion reaction period. Figure 2 shows the results from knockout experiments of a proton-transfer product (Figure 2a) and a protein−protein complex (Figure 2b). The experiment leading to Figure 2a involved the resonance ejection of the ubiquitin $U^{4+}$ proton-transfer product in the reaction of the $U^{8+}$ ion with the $U^{5-}$ ion. In the absence of resonance excitation, the $U^{4+}$ ion is the most abundant proton-transfer product. The significant result of the experiment leading to Figure 2a is that the acceleration and ejection of the $U^{4+}$ product during the ion/ion reaction period has no effect on the abundances of any of the other proton-transfer products or the $2U^{3+}$ product. Similarly, the acceleration of the $2U^{3+}$ product (Figure 2b) has no influence on the abundances of the proton-transfer products. These results are consistent with the conclusion that the major ion/ion reaction products observed under the conditions used in this work arise from single ion/ion encounters. The knockout experiments also indicate that none of the major products are long-lived intermediates (>1000 $\mu$s) in the formation of any other products. The time frame for ion acceleration is on the order of hundreds of microseconds such that any sequential processes that occur on that time frame or longer should be affected by the knockout experiment.

The relative contributions of proton transfer and complex formation to the product ion spectrum is dependent upon the charge states of the reactant ions as well as the identities of the reactants, as illustrated in Figures 3 and 4. Figure 3 compares

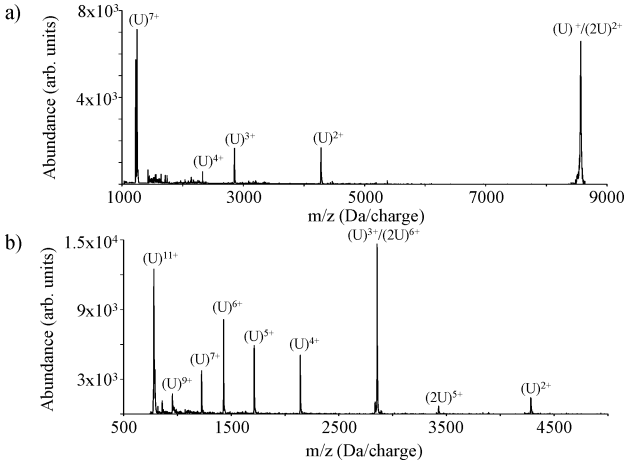


***Figure 3.*** Product ion spectra illustrating the results of ion/ion reactions between (a) 7+and 5− ions of ubiquitin (U) (120 ms reaction time) and (b) 11+ and 5− ions of ubiquitin (80 ms reaction time).

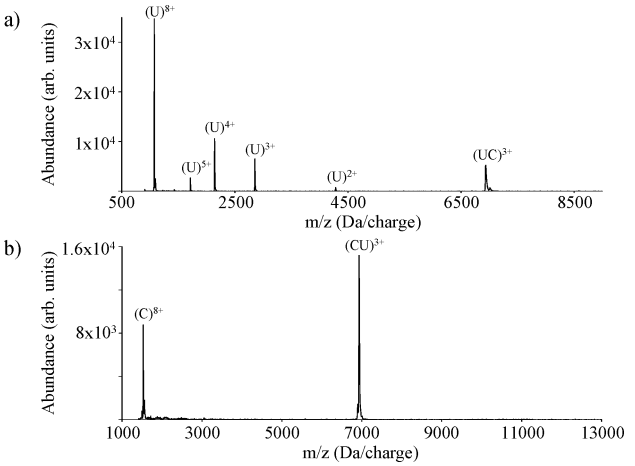


***Figure 4.*** Product ion spectra illustrating the results of ion/ion reactions between (a) 8+ ions of ubiquitin (U) and 5− ions of cytochrome *c* (C) and (b) 8+ ions of C and 5− ions of U. Both reactions progressed for 150 ms to yield the spectra shown. Note that this figure is adapted from the original communication (ref 10).

post-ion/ion reaction spectra of the ions $U^{7+}/U^{5-}$ (Figure 3a) and $U^{11+}/U^{5-}$ (Figure 3b). As a rule, the relative contribution of proton transfer products increases with the total absolute charge associated with the reactants, as reflected in the comparison of Figure 3. However, factors associated with the reactant proteins that have not yet been clearly identified can also play a significant role in determining the relative contributions of complex formation and proton transfer. Figure 4 compares data adapted from the original communication that compares the post-ion/ion reaction spectrum of $U^{8+}$ ions in reaction with $C^{5-}$ anions (Figure 4a) with the $C^{8+}$ ions in reaction with $U^{5-}$ anions (Figure 4b) under the same experimental conditions. The latter spectrum shows essentially no proton transfer products. In subsequent experiments, we have sometimes noted the appearance of low abundance proton transfer products with this reactant combination but they are consistently of much lower relative abundance than those arising from the reactant ion combination of Figure 4a. It is not yet clear why this reactant ion combination shows relatively little proton transfer. However, the collision cross-sections of the protein reactants may play a role (see the discussion of ion/ion reaction mechanisms).

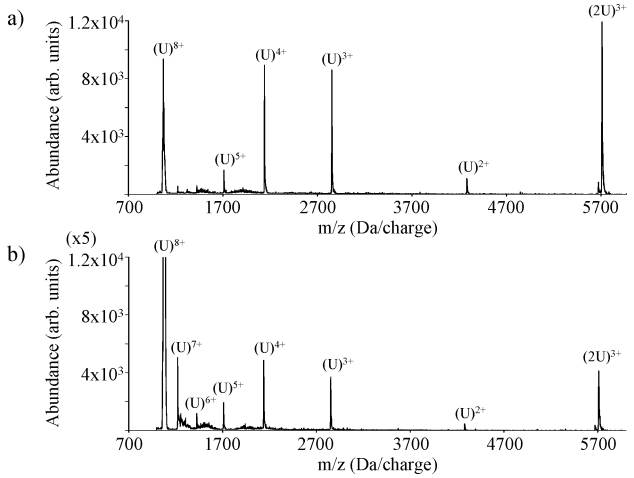


***Figure 5.*** Product ion spectra illustrating the results of ion/ion reaction between 8+ and 5− ions of ubiquitin (U) with a reaction time of (a) 84 ms and (b) 4 ms.

In measuring the overall ion/ion reaction rates, it was noted that at very short ion/ion reaction times products from one or two proton transfers were noted. This behavior is illustrated with the comparison of Figure 5, which shows post-ion/ion reaction spectra of $U^{8+}$ with $U^{5-}$ after 84 ms (Figure 5a) and 4 ms (Figure 5b) mutual ion storage times. Note that products corresponding to $U^{7+}$ and $U^{6+}$ are relatively abundant at the short reaction time and are largely absent at the longer reaction time. The appearance of products arising from a limited number of proton transfers is commonly observed when the spectrum is acquired shortly after the anion accumulation and isolation procedure. They tend to disappear with reaction time at roughly the same rate as the precursor ion after normalizing for charge (see below). This suggests that these products are not formed from the thermalized reactants. Rather, they are apparently formed from the reactants prior to the translational relaxation of the reactants after ion injection and isolation. After the reactants are thermalized via momentum transfer collisions with the helium bath gas, they are no longer formed and are lost via sequential reactions with the reactant ions of opposite polarity.

**Multiply Charged Ion/Ion Reaction Mechanisms.** The formation of protein−protein complexes via the reactions of multiply charged proteins of opposite polarities competes with varying degrees of proton transfer. Incomplete proton transfer is an interesting phenomenon because the full neutralization of the ion of lowest charge, either via complex formation or via proton transfer, is by far the thermodynamically preferred outcome. It is therefore clear that the processes that give rise to the product ion distributions are under kinetic control. Any model developed to rationalize and predict product ion distributions arising from reactions of multiply charged proteins of opposite polarity must account for the variety of phenomena presented above. These include the overall rates of reaction, the formation of protein−protein complexes, the distribution of incomplete proton-transfer products (i.e., both charge and abundance distributions), the role of total charge, and the role of relative translational energy. Furthermore, it is of interest to determine the key characteristics of the protein ions other than charge state that play roles in determining the relative contributions of complex formation and proton transfer (see Figures 3 and 4).

**Reaction Kinetics.** Several limiting cases can be identified in attempting to account for the observed overall reaction rates. These include "two-body" and "three-body" interactions. Trajectories can be bound or unbound. In the former case, the reactant ions assume elliptical orbits, presumably with a range of eccentricities, whereas in the latter case, the reactant ions assume hyperbolic or parabolic trajectories thereby undergoing deflection but not capture into a bound orbit. In the absence of a means for the removal of the initial relative translational energy of the reactants, two-body interactions lead to unbound trajectories. If a means for removal of the initial translational energy is active, such as collision with a third body, then the ions can assume a bound trajectory. In the case of protein ions moving under the influence of their mutual attraction, the possibility exists for interactions involving the direct physical contact of the proteins, interactions that allow for proton transfer without intimate contact of the proteins, and the formation of stable orbiting complexes that can lead to either proton transfer or physical collision.

One mechanism for complex formation is the direct "hard-sphere" collision between the reactant ions. The relationship between the hard-sphere collision radius, $r_{h-s}$, and the hard-sphere impact parameter, $b_{h-s}$, can be expressed as[22]

$$b_{h-s}{}^2 = r_{h-s}{}^2[1 + 2Z_1Z_2e^2/(4\pi\epsilon_0 r_{h-s}\mu v^2)] \quad (1)$$

where $Z_1$ and $Z_2$ are the unit charges on the ions, $e$ is the elementary charge, $\epsilon_0$ is the permittivity of vacuum, $\mu$ is the reduced mass of the collision pair, and $v$ is the relative velocity. A limited set of protein ion cross sections determined by ion mobility[4] and energy loss measurements[5] have been reported. These values can be used to provide initial estimates of the expected rates of reaction (see below), although it is not clear the extent to which the cross-sections of the ions might be affected by the approach of the oppositely charged ion.

The limiting case discussed above does not account for charge transfer over distances greater than the hard-sphere radius. (In the case of oppositely charged protein ions, charge transfer appears to take place via proton transfer, as opposed to electron transfer.) The relationship between the maximum distance over which a single proton transfer can occur, $r_{transfer}$, and the impact parameter for proton transfer, $b_{transfer}$, can be expressed as[22]

$$b_{transfer}{}^2 = r_{transfer}{}^2[1 + 2Z_1Z_2e^2/(4\pi\epsilon_0 r_{transfer}\mu v^2)] \quad (2)$$

The usual approach to estimate $r_{transfer}$ is to determine the distance at which the potential energy associated with the oppositely charged ion equals the reaction energy. In this case, the distance can be estimated as

$$r_{transfer} = Z_1Z_2e^2/(4\pi\epsilon_0\Delta G_{transfer}) \quad (3)$$

where $\Delta G_{transfer}$ is the free energy change associated with proton transfer between the relevant reactant ion pair. Ion/molecule reaction studies have provided a limited set of data for the dependence of the gaseous basicities of polypeptide ions on charge state[23] and these values can be used to determine an estimate of the reaction rates that might be expected (see below).

(22) Mahan, B. H. *Adv. Chem. Phys.* **1973**, *23*, 1−40.
(23) (a) Schnier, P. D.; Gross, D. S.; Williams, E. R. *J. Am. Chem. Soc.* **1995**, *117*, 6747−6757. (b) Cassady, C. J.; Wronka, J.; Kruppa, G. H.; Laukien, F. H. *Rapid Commun. Mass Spectrom.* **1994**, *8*, 394−400.

A third possible type of interaction is the three-body interaction first postulated by Thomson.[24] In this picture, the ionic reactants can form a bound orbit provided that the initial relative translational energy associated with the reactant pair is removed while the reactants are within a critical distance $d_{orbit}$. The maximum cross-section for the formation of a bound orbit, $\sigma_{orbit,max}$, is approximately given by[22]

$$\sigma_{orbit,max} \approx \pi {d_{orbit}}^2 \approx 4\pi {Z_1}^2 {Z_2}^2 e^4/[(4\pi\epsilon_0)(\mu v^2)^2] \quad (4)$$

The actual $\sigma_{orbit}$ is also determined by the probability that sufficient translational energy will be removed when the reactants are within the critical distance. Equation 4 is the limiting case for unit efficiency. The mechanism by which relative translation is removed is usually thought to be via collisions with a third-body. However, with such large ions, tidal processes[25] (e.g., the induction of intramolecular proton transfer as a result of the electric field of the oppositely charged ion) might play a significant role in determining the efficiency with which bound orbits are formed. Tidal effects, if significant, provide a means for the formation of a bound orbit in the absence of a third body. Another way of considering this possibility is that internal degrees of freedom of the ions serve as a sink for removal of relative translational energy of the ion pair. Furthermore, collisions and tidal effects can also lead to the collapse of the orbit to allow for either proton transfer or a physical collision to occur.

Under conditions in which the negative ions are in great excess, the reaction rates follow pseudo-first-order kinetics, that is

$$R_X = \pi {b_X}^2 \cdot v \cdot [\text{anions}] \quad (5)$$

where $X$ represents the type of interaction, viz., hard-sphere, proton transfer from an unbound trajectory, or formation of a bound orbit, and [anions] represents the effective anion number density. If the efficiency of formation of bound complexes is greater than a few percent, then the rates expected for the three types of processes increase in going from hard-sphere collisions to proton transfer via an unbound orbit to formation of an orbiting complex. Furthermore, if $r_{h-s}$ is independent of charge state, the hard-sphere collision cross-section for reaction is expected to increase linearly with reactant ion charge state. However, measurements of the physical cross-sections of proteins have shown that there is a tendency for cross-section, and thus $r_{h-s}$, to increase with charge. Hence, it might be expected that the hard-sphere collision rates will depend on $Z^n$ where $1 < n < 2$. Provided $\Delta G_{transfer}$ is independent of charge state, the cross-section for proton transfer from an unbound trajectory is expected to increase with the square of the charge. However, gas phase basicities (GB) of multiply charged anions and cations have been shown to vary with total ion charge due to intramolecular Coulomb repulsion.[23] The magnitude of $\Delta G_{transfer}$ is expected to increase with increasing reactant ion charge. Hence, it might be expected that rates for proton transfer from an unbound trajectory will depend on $Z^m$ where $1 < m < 2$. The cross-section for the formation of a bound orbit is independent of both the hard-sphere cross-section and $\Delta G_{transfer}$ and is therefore expected to increase with the square of the charge state.

***Table 1.*** Cross Section Data Taken for $11^+$–$3^+$ Taken from Ref 30[a]

| cyt c charge state | cross section (Å²) | $r_{h-s}$ (Å) | GB (kcal/mol) | $r'_{transfer}$ (Å) |
|---|---|---|---|---|
| 1 | 1125 | 18.92 | 240 | 24.44 |
| 2 | 1130 | 18.97 | 240 | 29.99 |
| 3 | 1139 | 19.04 | 228.5 | 32.92 |
| 4 | 1153 | 19.16 | 228.5 | 37.67 |
| 5 | 1196 | 19.51 | 216 | 39.2 |
| 6 | 1393 | 21.06 | 216 | 44.69 |
| 7 | 1785 | 23.84 | 205.9 | 48.45 |
| 8 | 1845 | 24.23 | 198.3 | 50.26 |
| 9 | 2215 | 26.55 | 192.5 | 54.25 |
| 10 | 2226 | 26.62 | 190.9 | 56.94 |
| 11 | 2303 | 27.08 | 184.5 | 58.58 |

[a] Cross-sections for $2^+$ and $1^+$ are estimates based on the trends noted for the measured cross-sections. GB values for charge states $11^+$-$3^+$ are taken from ref 23. GB values for the $2^+$ and $1^+$ charge states are assigned as 240 kcal/mol. The GB of the anion is assigned as 300 kcal/mol. The values used to calculate the cross-sections for proton transfer are referred to as $r'_{transfer}$ where $r'_{transfer} = r_{transfer} + r_{h-s}$. Use of $r'_{transfer}$ is equivalent to assuming that all of the protein charges are present on the surfaces of the protein ions nearest to the other reactant.

Previous experimental rate measurements of multiply charged proteins in reaction with singly charged perfluorocarbon anions in an ion trap indicated a dependence of the reaction rate on the square of the protein ion charge.[26] In measurements involving the singly charged perfluorocarbon anions, it is relatively straightforward to achieve the condition of excess negative charge such that pseudo-first-order kinetics is observed. We have yet to note a significant deviation from $Z^2$ dependence. However, the precision with which such measurements have been made does not preclude a rate dependence upon charge of slightly less than 2. Therefore, we have examined the predicted rate dependence upon protein charge for cytochrome *c* ions in reaction with singly charged anions of mass 400 Da at thermal energies (300 K) using the three cases outlined above. The values used for the hard-sphere collision and proton-transfer collision cases are listed in Table 1.

The absolute values for the cross-sections determined using the values listed in Table 1 and the relationships for the three interactions (eqs 1–4) are listed in Table 2.

The magnitudes of the calculated cross-sections can be used in eq 5 to determine the anion number density required to achieve a given reaction rate. For example, an ion/ion reaction rate for a $10^+$ protein ion with singly charged anions derived from perfluorocarbon anions derived from glow discharge ionization[26] is typically on the order of 500 $s^{-1}$ when a sufficient number of anions is admitted to show a small degree of resolution degradation for the anions due to space charge interactions. The anion number density required to achieve such a rate with the orbiting cross-section of Table 2 for $10^+$ cytochrome *c* is $(3-4) \times 10^7$ $cm^{-3}$, whereas it is roughly $2 \times 10^9$ $cm^{-3}$ for the cross-section determined for proton transfer via an unbound trajectory. The maximum anion number density under the conditions typically used in ion/ion reaction experiments, based on the Dehmelt pseudopotential well-depth

(24) Thomson, J. J. *Philos. Mag.* **1924**, *47*, 337–378.

(25) (a) Bates, D. R.; Morgan, W. L. *Phys. Rev. Lett.* **1990**, *64*, 2258–2260. (b) Morgan, W. L.; Bates, D. R. *J. Phys. B: At. Mol. Opt. Phys.* **1992**, *25*, 5421–5430.

(26) McLuckey, S. A.; Stephenson, J. L., Jr.; Asano, K. G. *Anal. Chem.* **1998**, *70*, 1198–1202.

***Table 2.*** Calculated Cross-Sections from Hard-Sphere, Proton Transfer, and Orbiting Complex Formation (unit efficiency for complex formation indicating an upper limit for bound orbit formation)

| charge state cyt c | hard sphere ($cm^2$) | proton transfer ($cm^2$) | orbit ($cm^2$) |
|---|---|---|---|
| 1 | $2.316 \times 10^{-12}$ | $3.033 \times 10^{-12}$ | $4.317 \times 10^{-11}$ |
| 2 | $4.53 \times 10^{-12}$ | $7.268 \times 10^{-12}$ | $1.727 \times 10^{-10}$ |
| 3 | $6.766 \times 10^{-12}$ | $1.184 \times 10^{-11}$ | $3.885 \times 10^{-10}$ |
| 4 | $9.039 \times 10^{-12}$ | $1.799 \times 10^{-11}$ | $6.907 \times 10^{-10}$ |
| 5 | $1.148 \times 10^{-11}$ | $2.331 \times 10^{-11}$ | $1.079 \times 10^{-9}$ |
| 6 | $1.485 \times 10^{-11}$ | $3.185 \times 10^{-11}$ | $1.554 \times 10^{-9}$ |
| 7 | $1.961 \times 10^{-11}$ | $4.023 \times 10^{-11}$ | $2.115 \times 10^{-9}$ |
| 8 | $2.276 \times 10^{-11}$ | $4.761 \times 10^{-11}$ | $2.763 \times 10^{-9}$ |
| 9 | $2.805 \times 10^{-11}$ | $5.778 \times 10^{-11}$ | $3.496 \times 10^{-9}$ |
| 10 | $3.122 \times 10^{-11}$ | $6.733 \times 10^{-11}$ | $4.317 \times 10^{-9}$ |
| 11 | $3.491 \times 10^{-11}$ | $7.612 \times 10^{-11}$ | $5.223 \times 10^{-9}$ |

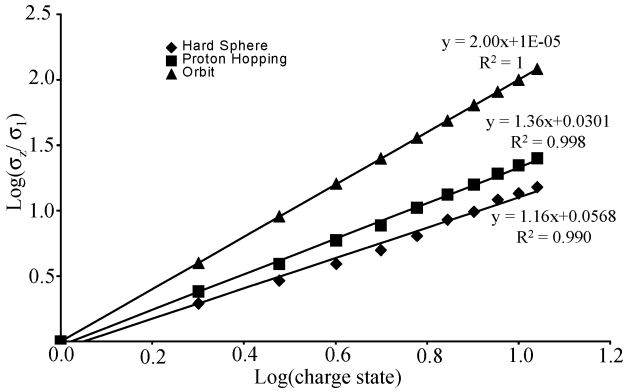


***Figure 6.*** Plots of the logarithm of the predicted cross-section versus the logarithm of the charge of the cytochrome *c* ion for hard-sphere collisions, proton transfer, and stable orbit formation based on eqs 2−4 and the data in Tables 1 and 2.

model,[27] is roughly an order of magnitude lower than that necessary for the proton-transfer reaction. This suggests that orbiting interactions are needed to explain the magnitudes of the ion/ion reaction rates observed in the ion trap.

The *Z*-state dependences of the three types of interactions also provide insights into the role of orbiting collisions. Figure 6 shows a plot of the logarithm of the predicted cross-section versus the logarithm of the charge of the cytochrome *c* ion for the three cases. The slopes of the lines give the predicted *Z*-state dependences. In the case of the hard-sphere collision picture, the cross-section increases with $Z^n$ where *n* is roughly 1.16. The trend is not strictly linear as the cross-section dependence upon *Z* is not linear. In the proton-transfer case, the cross-section increases as $Z^n$ where *n* is between 1.3 and 1.4. Some scatter is associated with the plot because the values of $\Delta G_{transfer}$ do not follow a strictly linear dependence on charge. In the case of bound orbit formation, the cross-section dependence goes strictly as the square of the charge ($n = 2$). The experimentally observed *Z*-dependencies for multiply charged proteins in reactions with singly charged perfluorocarbon anions is most consistent with the formation of bound orbits being rate-determining.

Rates for ion/ion reactions where both ion polarities are formed by nano-ES are generally more difficult to measure than

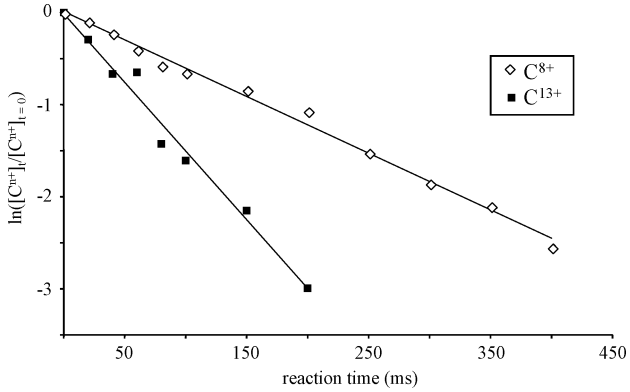


***Figure 7.*** Reaction rate data ($\ln([\text{positive reactant}]_t/[\text{positive reactant}]_{t=0})$ versus reaction time, *t*) collected for the reactions of 13+ and 8+ cytochrome *c* ions with 5− cytochrome *c*. The data were collected with an excess of 5− ions to ensure pseudo-first-order kinetics for the disappearance of the positive reactant. For the 8+/5− reaction, a straight line fit yields a slope of 6.2 $s^{-1}$, with a correlation coefficient ($R^2$) of 0.993. For the 13+/5− reaction, the slope is 14.9 $s^{-1}$ and the $R^2$ is 0.98.

those involving singly charged ions derived via glow discharge due to greater fluctuations in ion signals with time using nano-ES for both ion polarities. For this reason, reaction rates for only a few combinations of positive and negative ion charge states have been measured thus far. Figure 7 shows a comparison of rate data collected for the $C^{13+}$ and $C^{8+}$ cations with $C^{5-}$ anions under conditions where the total anion charge was in great excess over the total positive ion charge. Therefore, the loss of the positive ions followed pseudo-first-order kinetics. Overall rates of reaction for the higher and lower positive ion charge states were 14.9 $s^{-1}$ and 6.2 $s^{-1}$, respectively. Under conditions of constant $v \cdot [C^{5-}]$, which applies in this case, the predicted ratio of the rates of the $C^{13+}$ and $C^{8+}$ ions with $C^{5-}$ ions from eq 4 is 2.6 and the experimental ratio is 2.4. On the basis of the predicted charge state dependence of $Z^{1.36}$ for the proton transfer model, as derived from Figure 6, this rate ratio is expected to be 1.9. Therefore, the rates for the multiply charged protein reactions suggest that the formation of stable orbiting complexes is involved under the conditions of this study.

**Proton Transfer vs Complex Formation.** Several models have been considered to rationalize incomplete proton transfer and its competition with complex formation. One model assumes that all products arise from a single excited chemically bound complex intermediate, as described in the original communication. In this picture, up to all of the potential energy associated with mutual neutralization is available to drive decomposition of the complex into all of the various complementary charge state combinations. The complex can be formed by a direct hard-sphere collision, a relatively low cross-section process, or via the collapse of a bound ion/ion orbit. The former case makes much of the initial potential energy available to drive charge separation reactions. In the latter case, at least some of the initial potential energy can be dissipated by collisions that lead to collapse of the orbit. Upon the initial formation of the complex, proton transfer between the reactants proceeds in parallel with radiative and collisional cooling of the complex and decomposition of the complex. The product ion distribution is determined by the kinetics associated with proton transfer between the protein subunits, unimolecular decomposition of the complex

(27) March, R. E.; Hughes, R. J. *Quadrupole Storage Mass Spectrometry*; John Wiley & Sons: New York, 1989.

with its various distributions of charge between the subunits, and removal of excess energy via ion/helium collisions.

A kinetic scheme for this "unimolecular" model is shown in Scheme 1 for the reaction of $C^{8+}$ cations with $C^{5-}$ anions:

***Scheme 1.*** "Unimolecular" Kinetic Scheme

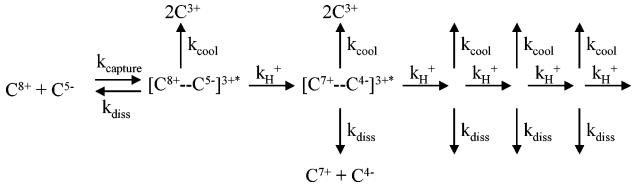


The intramolecular proton transfer reactions are taken to be essentially irreversible due to the high exothermicity associated with charge neutralization. If it is assumed that the overall rate-limiting process is the formation of the complex (i.e., $[(C^{8+} - C^{5-})^{3+*}]_0 = 1$), rate expressions can be derived to determine the relative abundances of the reaction products, provided the relevant rate constants are known. Figure 8 shows the post-ion/ion reaction positive spectrum resulting from the $C^{8+}/C^{5-}$ reaction after a mutual storage time of 100 ms. Assuming a cooling rate constant of 100 $s^{-1}$ for all $k_{cool}$,[28] the relative abundances could be fitted to the abundances of the experimental data with the proton transfer and dissociation rate constants listed in the figure insert. The circles at the tops of the peaks represent the calculated relative abundances with a given set of proton transfer and dissociation rate constants. Excellent fits to the experimental data can be made with a large number of proton transfer and dissociation rate combinations; however, in all cases where the cooling rates are kept between 100 and 1000 $s^{-1}$, the rate constants for intra-complex proton transfer and the unimolecular dissociation rate constants appear to be orders of magnitude lower than expected. With such low dissociation rate constants, the knockout experiment of Figure 2b would be expected to affect the abundances of the proton-transfer products. Furthermore, the various $k_{diss}$ values were chosen arbitrarily to fit the spectrum, but there is no apparent a priori rationale for choosing dissociation rates that peak at the intermediate charge state combinations. Another possible inconsistency with this model is the absence of evidence for amide bond cleavage. Such unimolecular reactions might be expected to compete with the various charge separation channels if all processes take place from a chemically bound complex. Therefore, this model does not seem to account reasonably well for all of the phenomenology thus far noted for protein anion/protein cation reactions.

The model described above does not account for the possibility for proton transfer at distances greater than those associated with intimate complex formation. A second limiting model assumes that all products are formed either by proton transfer reactions (without complex formation) or complex formation via hard-sphere collisions. This picture is immediately called into question by the fact it does not appear to account for the overall reaction rates. However, in the absence of accurate and precise ion number densities, it is useful to consider this picture to determine if it can account, at least qualitatively, for the relative abundances of the product ions. A distinct kinetic scheme can be drawn for this picture, as illustrated in Scheme 2:

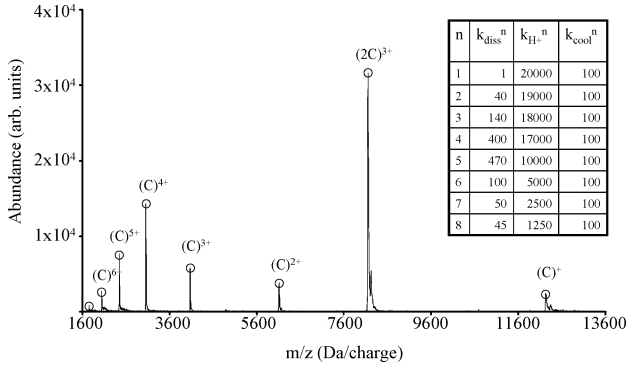


***Figure 8.*** Product ion spectrum resulting from the reaction of 8+ and 5- cytochrome *c* (C) for 100 ms (data presented previously in ref 10). The open circles at the tops of the peaks represent the relative product ion abundances calculated using the kinetic expressions given in the text, assuming a cooling rate constant of 100 $s^{-1}$ for all $k_{cool}^n$ and using the values for $k_{diss}^n$ and $k_{H+}^n$ given in the inset table.

***Scheme 2.*** "Proton Hopping" Kinetic Scheme

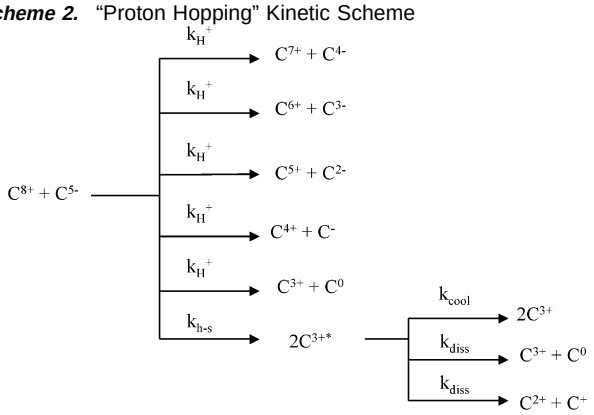


In Scheme 2, the various proton transfer channels are indicated as competitive processes. This is likely to be an oversimplification in that multiple proton transfers are likely to occur in sequence as the collision partners approach one another. However, if they occur on a single encounter, the use of a single rate is appropriate. (In this scheme, all of the $C^{2+} + C^{+}$ products are indicated as arising from unimolecular dissociation of $2C^{3+}*$. This is because the formation of this product ion pair is only likely to occur over distances associated with proton transfer from an ion to a neutral molecule.) Figure 9 compares the post-ion/ion reaction positive spectrum resulting from the $C^{8+}/C^{5-}$ reaction (see also Figure 8) with predicted relative abundances based in Scheme 2 and the relative proton-transfer rate constants listed in the figure insert. The relative proton-transfer rate constants are consistent with the cross-sections for proton transfer listed in Table 2. In this simulation, the GB values of the cytochrome *c* anions are taken to change by 5 kcal/mol/Z from a value of 300 kcal/mol for the −1 anion. To predict the abundances in the spectrum of the products formed via competitive processes, the cross-section for $C^{8+}/C^{5-} \rightarrow C^{7+}/C^{4-}$ was taken as the difference between the $C^{8+}/C^{5-} \rightarrow C^{7+}/C^{4-}$ and $C^{7+}/C^{4-} \rightarrow C^{6+}/C^{3-}$ cross-sections. The abundances of the other competitive proton-transfer products were determined in like fashion. The cross sections for the formation of the $2C^{3+}*$ species and the $C^{3+}/C^{0}$ species were

(28) Goeringer, D. E.; McLuckey, S. A. *Int. J. Mass Spectrom.* **1998**, *177*, 163–174.

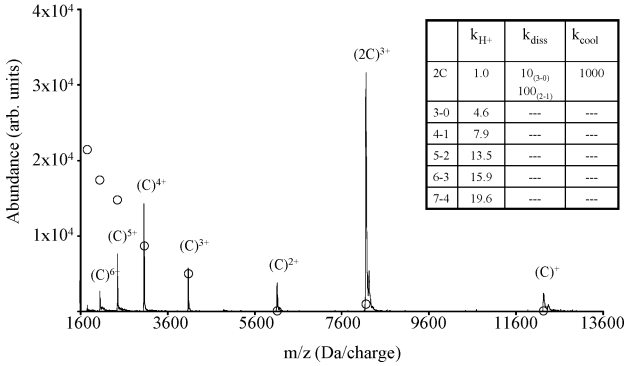


***Figure 9.*** Post-ion/ion reaction positive spectrum resulting from the $C^{8+}/C^{5-}$ reaction (see also Figure 8) with predicted relative abundances based in Scheme 2 and the rate constants listed in the insert. The values of the proton-transfer rate constants relative to one another consistent with the cross-sections for proton transfer listed in Table 2.

determined by extrapolating the rate of change from the previous steps. (A cooling rate of 1000 $s^{-1}$ and dissociation rates of 100 and 1000 $s^{-1}$ were chosen arbitrarily. The main objective of this exercise was to determine the degree to which the proton-transfer products could be modeled with this picture. The relative abundances of the $C^{2+}$ and $C^{+}$ ions are of secondary interest.) This model predicts decreasing abundances as charge decreases for the $C^{7+}$, $C^{6+}$, $C^{5+}$, and $C^{4+}$ products. It also predicts much less complex would be formed than is found in the experimental data. Therefore, this picture does not approximate well either the shape of the charge state abundance distribution or the magnitude of the abundance of the complex.

A third model takes into account the formation of an orbiting complex as the rate determining step and allows for proton-transfer reactions and collapse into a chemical complex. Equation 4 provides a relationship for determining the maximum cross-section for the formation of a stable orbiting complex. As indicated above, this relationship accounts for the charge-squared dependence of the reaction rate and the magnitude of the calculated cross-section is large enough to account for the measured reaction rates with the ion number densities expected in the ion trap. Proton transfer reactions followed by separation of the products might be expected to occur through elliptical orbits that bring the reactants into close proximity such that the attractive electric field can induce proton transfer without the formation of a chemically bound complex. If the transfer of protons occurs without a large change in the relative translation of the particles, then some of the products can escape from one another as a result of the decrease in the mutually attractive electric field resulting from the charge transfer. If the ions do not escape from one another, then the orbit will tend to collapse due to collisions and tidal effects thereby allowing for additional proton transfer and, in some cases, condensation of the ions into a chemically bound complex. The tendency for separation of proton transfer products is expected to increase as the total charge of the products decreases due to the decrease in the mutually attractive Coulomb field. Once the reactants approach distances where a physical collision can occur, the likelihood for complex formation is greatest. Complexes can be formed via either bound or unbound orbits. Formation of complexes via bound orbits can occur over a wide range of relative translational energies because of the range of possible eccentricities. In the case of the $U^{8+}$ ion, cross-sections of 1442 $Å^2$ and 1622 $Å^2$ have been reported,[29] and in the case of the $C^{5-}$ ion, the reported cross section is 1246 $Å^2$.[30] Hence, the nominal diameters of the protein ions in this study are on the order of 40−50 Å, which is the same order of distance over which the electric fields can be large enough to favor proton transfer. Hence, as the reactants increase in size and decrease in charge, the fraction of low impact parameter collisions that lead to proton transfer without undergoing a physical collision decreases. This trend is reinforced by the increase in proton binding strengths as charge state decreases.[23] Hence, in this picture, partial proton-transfer products are expected to increase in relative abundance as the charges of the ions increase, as is observed. The formation of complexes is expected to increase with the cross-section for physical collisions.

A third distinct kinetic scheme applies to the orbiting ion/ion interaction case. Scheme 3 provides a simple representation of the process:

***Scheme 3.*** "Orbital Complex" Kinetic Scheme

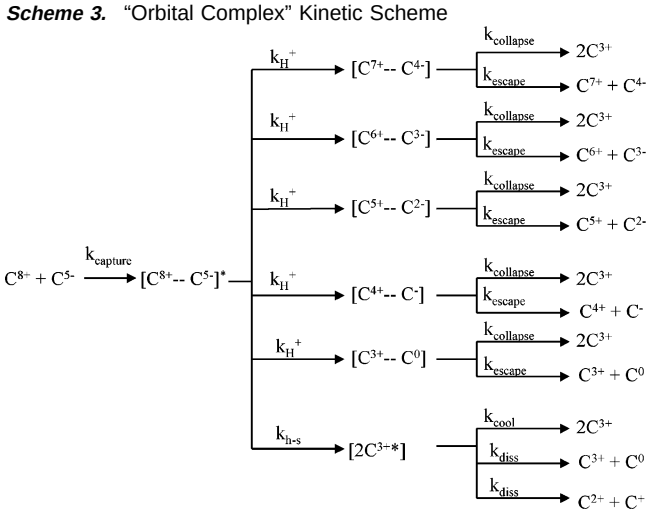


The overall rate is determined by the formation of a Coulombically bound complex. Proton transfer reactions can occur within this complex as well as a physical collision between the partners. Each of the first generation products can "escape" their mutual attraction into separated proton transfer products or they can eventually "collapse" to a stable chemically bound complex. In this scheme, the relative proton-transfer rates might be expected to show the *Z*-dependence similar to that predicted by eq 2 (see Figure 6). The relative $k_{escape}$ values, on the other hand, might be expected to be inversely related to squares of the charges on the proton-transfer product ions. This situation gives rise to two competing tendencies. The likelihood for proton transfer increases with increasing total charge, whereas the likelihood for the separation of the proton-transfer products decreases with increasing total charge. These competing tendencies may account for the shape of the abundance distribution of the proton-transfer products.

Figure 10 shows the data for the $C^{8+}/C^{5-}$ reaction along with predicted abundances based in Scheme 3 and rate constants based on eq 2, eq 4, and cytochrome *c* cation GB values listed in Table 1. Anion GB values were taken as those used above to determine relative abundances from Scheme 2. The rate

(29) Valentine, S. J.; Counterman, A. E.; Clemmer, D. E. *J. Am. Soc. Mass Spectrom.* **1997**, *8*, 954−961.
(30) Shelimov, K. B.; Clemmer, D. E.; Hudgins, R. R.; Jarrold, M. F. *J. Am. Chem. Soc.* **1997**, *119*, 2240−2248.

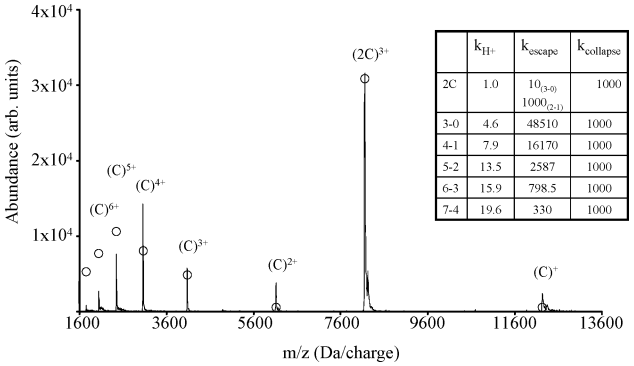


| | $k_{H^+}$ | $k_{escape}$ | $k_{collapse}$ |
|---|---|---|---|
| 2C | 1.0 | $10_{(3-0)}$ $1000_{(2-1)}$ | 1000 |
| 3-0 | 4.6 | 48510 | 1000 |
| 4-1 | 7.9 | 16170 | 1000 |
| 5-2 | 13.5 | 2587 | 1000 |
| 6-3 | 15.9 | 798.5 | 1000 |
| 7-4 | 19.6 | 330 | 1000 |

***Figure 10.*** Post-ion/ion reaction positive spectrum resulting from the $C^{8+}/C^{5-}$ reaction (see also Figure 8) along with predicted abundances based in Scheme 3 and rate constants based on eq 2, eq 4, and cytochrome *c* GB values listed in Table 1. The rate constants for cooling were all taken to be 1000 $s^{-1}$. The relative proton-transfer rate constants listed in the figure were determined in direct analogy with the procedure used to determine the relative rate constants for proton transfer for Figure 9, as described above. The rate constants for escape of the proton-transfer products from a stable orbit relative to one another were based on the eq 4 (see text).

constants for collapse and cooling were all taken to be 1000 $s^{-1}$. The relative proton transfer rate constants listed in the figure were determined using the same procedure used to determine the relative rate constants for proton transfer for Figure 9, as described above. The relative escape rate constants associated with the bound orbiting complexes were chosen to be inversely related to the square of the product ion charges for the cases in which both products are charged. The value for escape of the 3−0 pair was set to about 3 times that of the 4−1 pair, as the attractive potential associated with the products is no longer dominated by the long-range Coulomb potential. The dissociation values for $2C^{3+}$ were arbitrarily chosen, as with the comparison of Figure 9. The relative rate constants were scaled to obtain the best fit to the data. The restrictions imposed by use of the experimental GB data and the predicted charge-dependent trends for proton transfer and escape from the orbiting complexes does not allow for an excellent fit to the data, unlike the comparison of Figure 8, in which no restrictions were placed on the rate constants used to fit the data. However, this picture better reproduces the observed distribution of charge-transfer products and the relative abundance of the protein−protein complex than does the picture based in Scheme 2. The simulation of Figure 10 is obviously based upon rather crude approximations and simplifications. Furthermore, the dynamics associated with the collapse of the orbiting complex may also show a charge state dependence, which is not accounted for in this simulation. Nevertheless, the results obtained here are taken as an indication that the picture associated with Scheme 3 best accounts for ion/ion product distribution resulting from reactions that occur after both ion populations are collisionally stabilized to the center of the ion trap.

**One and Two Proton Transfers at Short Reaction Times.** The observation of one and two proton transfer products at short reaction times is noteworthy in that a significantly different distribution of relative abundances of proton transfer products is observed once the two ion populations have been collisionally stabilized to the center of the ion trap. The observation that these proton transfer products do not increase (in fact, they tend to react away) with mutual ion storage time suggests that they may be formed from reactant ions of relatively high translational

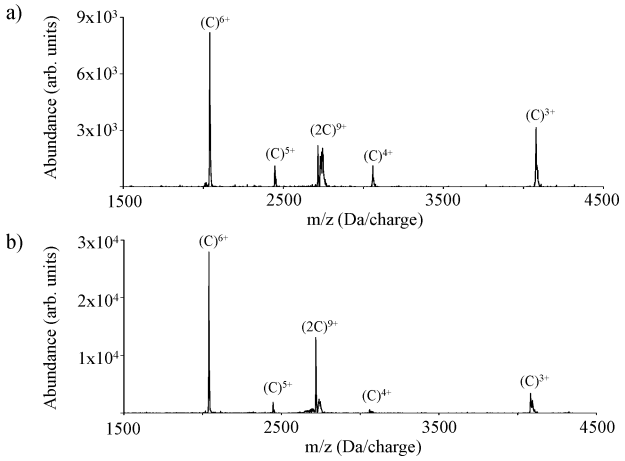


***Figure 11.*** Product ion spectra resulting from ion trap collisional activation of isolated 9+ bovine cytochrome *c* homodimers formed by various means. (a) Collsional activation of the 9+ homodimer formed in the gas-phase via reaction of 15+ and 6- cytochrome *c* ions. (b) Collisional activation of the 9+ homodimer formed via electrospray of a 1.0 mg/mL bovine cytochrome *c* solution in pure water. The 11+ dimer was isolated in the trap, and the charge state was reduced to 9+ via reactions with anions of PDCH generated by corona discharge ionization. This 9+ dimer was then isolated and collisionally activated to yield the spectrum shown.

energy. Such ions are present during the ion accumulation period and for a short time after ion accumulation and ion isolation. The efficiency of ion accumulation into the ion trap is on the order of a few percent.[31] Therefore, during the ion accumulation period, there is a larger steady state number of ions of the polarity being injected than is present after the accumulation period ends. These ions are of higher translational energy, however, than the collisionally stabilized trapped ions. It might be significant that the cross-section for proton transfer (see eq 2) is inversely related to the square of the relative velocity whereas the cross-section for the formation of a stable orbit is inversely related to the fourth power of the relative velocity. Therefore, it is expected that increasing the relative velocities of the reactants will favor proton transfer as the major process. Therefore, the one and two proton transfer products observed when mass analysis takes place very shortly after the accumulation of the second ion population is consistent with the proton-transfer process described by eq 2 and Scheme 2.

**Characterization of Protein/Protein Complexes via Tandem Mass Spectrometry.** Having recognized that protein−protein complexes can be synthesized in the gas phase, an obvious question arises regarding the structures and stabilities of these products, particularly in relation to the nominally identical complexes formed from solution. We have examined various charge states of ubiquitin and cytochrome *c* homodimers as well as mixed dimers of the two proteins synthesized in various ways. A limited subset of results is reported here that summarizes the main phenomenology noted for protein dimer ions.

Figure 11a shows the product ion spectrum produced from the ion trap collisional activation of the 9+ bovine cytochrome *c* homodimer produced from the reaction of the $C^{15+}$ cation and the $C^{6-}$ anion. $2C^{9+}$ homodimer ions were produced via several other charge state combinations and all product ion

(31) (a) Appelhans, A. D.; Dahl, D. A. *Int. J. Mass Spectrom.* **2002**, *216*, 269−284. (b) Quarmby, S. T.; Yost, R. A. *Int. J. Mass Spectrom.* **1999**, *190/191*, 81−102.

spectra produced via ion trap collisional activation were very similar to that of Figure 11a (data not shown). The major product ions show an asymmetrical distribution of the product charges whereby most product signal is partitioned into the complementary pair of $C^{6+}/C^{3+}$ ions. The more symmetrical charge distribution of $C^{5+}/C^{4+}$ is also observed but at much lower abundance. Figure 11b shows the product ion spectra derived from the 9+ homodimer of bovine cytochrome *c* formed via electrospray and shows very similar behavior to that of the complex formed in the gas phase. There appears to be somewhat more of a contribution from the minor product channel, viz. $C^{5+}/C^{4+}$, in the gas-phase spectrum but this higher abundance was not consistently observed for all of the gas phase complexes. Similar asymmetric product ion charge distributions from dissociation of multiply charged noncovalent complexes have been reported when ions are formed in the condensed phase.[1c,3] The extent to which asymmetry is observed in the distribution of product ion charge tends to increase with the total charge of the complex and on characteristics of the subunits such as conformational flexibility. This phenomenon appears to be related to the dynamics of dissociation.[3e,32] Upon activation, one of the subunits tends to unfold and, by virtue of the greater separation of charge sites, can accommodate more charge. Proton transfer into the more extended subunit can occur resulting in an asymmetric distribution of charges in the products. It is noteworthy that the underlying factors that give rise to asymmetric product ion charge distributions from protein complexes formed in solution also appear to apply to the complexes formed in the gas phase by ion/ion reactions.

A unique capability of the ion/ion reaction approach to forming gaseous protein−protein complexes is that there is a high degree of control over the identities of the reactants. This is illustrated in the comparison of Figure 12, which compares the dissociation behavior of 9+ heterodimers of bovine and equine cytochrome *c* (E) formed by different means. Two homologous proteins were chosen to provide a mass difference to allow for ready distinction of the subunits but to otherwise minimize differences. The product ion spectrum from the dissociation of the heterodimer formed initially in solution is shown in Figure 12a. The most abundant charge state formed was the $CE^{11+}$ ion. Relatively little $CE^{9+}$ ion was formed in solution. To collect a self-consistent set of data, the $CE^{11+}$ ion was converted to the $CE^{9+}$ ion via two consecutive proton-transfer reactions with anions derived from glow discharge ionization of PDCH. As noted with the bovine cytochrome *c* homodimer, the $CE^{9+}$ heterodimer fragments largely to the 6+/3+ products. Within experimental error, there appears to be no preference between the bovine and equine versions of the protein for either product ion charge state. That is, equal abundances of both possible complementary sets of ions, $C^{6+}/E^{3+}$ and $E^{6+}/C^{3+}$, are observed. Figure 12b shows the product ion spectrum from the $CE^{9+}$ complex formed in the gas phase by reacting $C^{15+}$ cations with $E^{6-}$ anions. Once again, the asymmetric charge distribution is observed. However, there is a strong preference for dissociation into the $C^{6+}/E^{3+}$ complementary pair of products. Figure 12c shows the product ion spectrum derived from the $CE^{9+}$ complex formed in the gas phase by reaction of $E^{15+}$ cations with $C^{6-}$ anions. This $CE^{9+}$ complex shows the

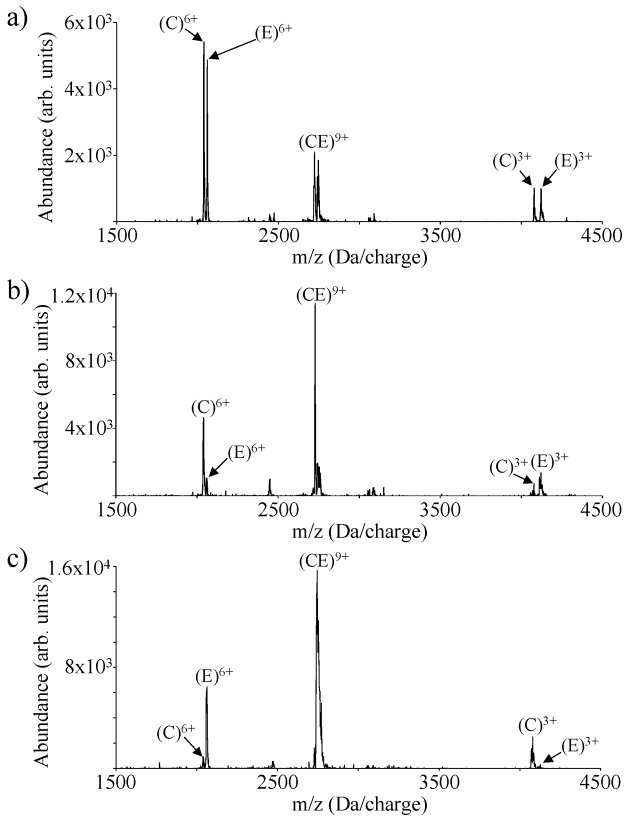


***Figure 12.*** Product ion spectra resulting from ion trap collisional activation of the isolated 9+ bovine/equine cytochrome *c* heterodimers formed by various means. (a) Collisional activation of the 9+ bovine/equine heterodimer formed via electrospray of a solution containing 0.5 mg/mL of each protein in pure water. The 11+ heterodimer was isolated and reduced to 9+ via reaction with anions of PDCH generated by corona discharge ionization. This 9+ heterodimer was then isolated and collisionally activated to yield the spectrum shown. (b) Collsional activation of the 9+ heterodimer formed in the gas-phase via reaction of 15+ bovine cytochrome *c* ions (C) with 6- equine cytochrome *c* ions (E). (c) Collsional activation of the 9+ heterodimer formed in the gas-phase via reaction of 15+ equine cytochrome *c* ions (E) with 6- bovine cytochrome *c* ions (C).

opposite behavior to that of the heterodimer of Figure 12b. In this case, $E^{6+}$ is the dominant 6+ product whereas $C^{3+}$ is the dominant 3+ product. Clearly, in the gas phase experiment, the products display a memory of how the complex was formed. The observed behavior cannot be readily explained by the small differences in the sequences of the two proteins. However, the results may very well be consistent with the idea that the least compact subunit will tend to accrue most of the charge in asymmetric break-up of the complex. The reported gas-phase cross-sections of the $C^{15+}$ and $C^{6-}$ ions of cytochrome *c* are 2579 Å$^2$, and 1244−1535 Å$^2$ (several conformations of different cross-section could be resolved for the 6- ion), respectively.[30] Provided similar cross-sections apply to the ions used to form the $CE^{9+}$ complex, the cationic reactant is significantly less compact than the anionic reactant. If this relative size difference is maintained within the complex, then it is expected that the cationic reactant would retain most of the positive charge upon dissociation. If this interpretation is correct, then it indicates that the dissociation behavior of protein complexes formed in the gas-phase can be used to probe characteristics of the subunits used to synthesize them. An alternative interpretation is that the time required for full isomerization of the protons between the complex components is slow relative to the hundreds of

(32) Jurchen, J. C.; Williams, E. R. *Proceedings of the 50th ASMS Conference on Mass Spectrometry and Allied Topics*; June 2−6, Orlando, FL.

milliseconds time frame of the ion trap experiment. In any case, this result highlights the control over the synthesis of gaseous complexes that the ion/ion reaction approach affords.

## Conclusions

Reactions of oppositely charged protein ions in the gas phase gives rise to the formation of protein−protein complexes and a series of proton transfer products via single reactant ion encounters. The relative abundances of the proton transfer products tend to maximize between the extremes of single proton transfer and full proton transfer. A mechanism that gives rise to single and double proton transfers is apparent at short reaction times and may arise from reactant ions that are not yet thermalized in the ion trap environment. No fragmentation of covalent bonds associated with the protein reactants has yet been noted. The relative contributions of proton transfer and complex formation are determine by the charges on the reactants and, possibly, by their physical cross-sections. The formation of a stable orbiting complex appears to be rate-limiting in the case of multiply charged cytochrome *c* ions of opposite polarity. A model whereby all ion/ion reaction products arise from a single excited chemically bound protein complex appears to suffer from the requirement of very low intramolecular proton transfer rates and unimolecular dissociation rates to account for experimental observations. A model that only allows for two-body interactions without formation of bound orbits does not appear to account for either the magnitudes of the rates or the relative abundances of the products. A model that allows for proton transfer and complex formation via bound orbits appears to show the greatest promise in accounting for experimental observations. The relatively limited set of observations of the dissociation of protein complexes formed in the gas phase indicates similar behavior to those formed in solution. However, the gas phase complexes can be synthesized in various ways and the dissociation behavior can retain memory of how the complex is synthesized. The ability to synthesize protein complexes from well-characterized subunits can be may prove to be helpful in understanding the gas phase behavior of protein complex ions formed initially in solution.

**Acknowledgment.** This research was sponsored by the National Institutes of Health under Grant GM45372 and the U.S. Department of Energy under Award No. DE-FG02-00ER15105.

JA035051L